Density Functional Theory Study of the Reaction Mechanism for Competitive Carbon−Hydrogen and Carbon−Halogen Bond Activations Catalyzed by Transition Metal Complexes†

Xinzheng Yang and Michael B. Hall*

Department of Chemistry, Texas A&M University, College Station, Texas 77843-3255

Received: October 20, 2008; Revised Manuscript Received: December 9, 2008

Carbon−hydrogen and carbon−halogen bond activations between halobenzenes and metal centers were studied by density functional theory with the nonempirical meta-GGA Tao−Perdew−Staroverov−Scuseria functional and an all-electron correlation-consistent polarized valence double-ζ basis set. Our calculations demonstrate that the hydrogen on the metal center and halogen in halobenzene could exchange directly through a kite-shaped transition state. Transition states with this structure were previously predicted to have high energy barriers (*J. Am. Chem. Soc.* **2005**, *127*, 279), and this prediction misled others in proposing a mechanism for their recent experimental study (*J. Am. Chem. Soc.* **2006**, *128*, 3303). Furthermore, other halo−carbon activation pathways were found in the detailed mechanism for the competitive reactions between cationic titanium hydride complex $[Cp^*(^tBu_3P{=}N)TiH]^+$ and chlorobenzene under different pressure of H_2. These pathways include the *ortho*-C−H and Ti−H bond activations for the formation and release of H_2 and the indirect C−Cl bond activation via β-halogen elimination for the movement of the C_6H_4 ring and the formation of a C−N bond in the observed final product. A new stable isomer of the observed product with a similar total energy and an unexpected bridging between the Cp* ring and the metal center by a phenyl ring is also predicted.

1. Introduction

Development of more active and selective activation catalysts for aryl−hydrogen and aryl−halogen bonds is essential for many transition metal catalyzed protocols.[1] As a highly reactive class of compounds, organotitanium hydrides have been implicated in a variety of catalytic processes and studied widely in recent years.[2,3]

In a recent study of the C_6H_5−H and C_6H_5−X (X = Cl, Br) bond activations in halobenzenes at cationic titanium centers, Ma et al.[3] reported a number of interesting halogen activation products depending on the amount of H_2 present in the reaction medium. At about 4 atm of H_2, they observed the exchange of H and X in the reaction between MH^+ (**1,** M = $Cp^*(^tBu_3P{=}N)Ti$) and C_6H_5X to produce MX^+ (**2X**) and C_6H_6 (Scheme 1). At lower H_2 pressure (still >1 atm), they observed the release of H_2 through *ortho*-C−H activation and the formation of the β-halophenyl cation $M(2\text{-}X{-}C_6H_4)^+$ (**3X**). While in the absence of H_2, they observed that the most stable isomer $MX(C_6H_4)^+$ (**4X**) apparently transformed from **3X** through the β-halogen elimination reaction by moderate heating. To explain the hydrogen−halogen interchange reaction in this cationic Ti system, Ma et al.[3] proposed a reaction pathway that invokes nucleophilic attack on the aryl halide followed by β-halo transfer to the metal, a pathway that avoided proposing the concerted kite-shaped transition state (**I**) because Maron et al.[4] in a previous theoretical study of the H/F exchange between Cp_2La and C_6F_6 could not find such a transition state and postulated that it is energetically unfavorable. For the formation of the final product **4X** through the β-halogen elimination reaction of **3X**, Ma et al.[3] also proposed a transition state where the rotation of the phenyl ring breaks the C−Cl bond and forms a C−N bond simultaneously. To examine two issues, (1) the existence of this kite-shaped transition state for H/X exchange and (2) the phenyl rotation transition state for the formation of **4X** from **3X**, we performed some preliminary calculations using density functional theory (DFT), and we were surprised to find a low-energy kite-shaped transition state for H/Cl exchange between C_6H_5Cl and **1**. Meanwhile, all searches for the phenyl rotation transition state for the formation of **4X** from **3X** failed after many attempts. These results prompted us to reexamine the H/F exchange in the La system, where Maron et al. predicted that the kite-shaped transition state was high in energy, to determine the real mechanism for the H/X exchange for both

SCHEME 1

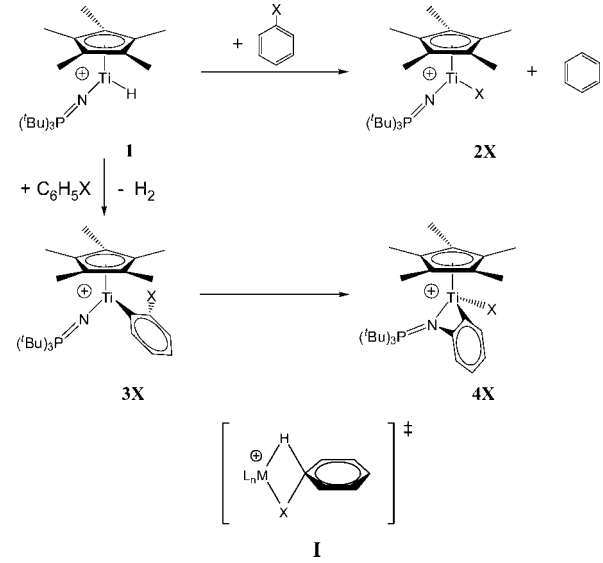

† Part of the "Max Wolfsberg Festschrift".

* To whom correspondence should be addressed. E-mail: mbhall@tamu.edu.

10.1021/jp809272y CCC: $40.75
Published on Web 01/23/2009

SCHEME 2: Predicted Reaction Pathway of the Direct Exchange of H/F between Cp_2LaH and C_6F_6 through a Kite-Shaped Transition State $TS_{B,C}$

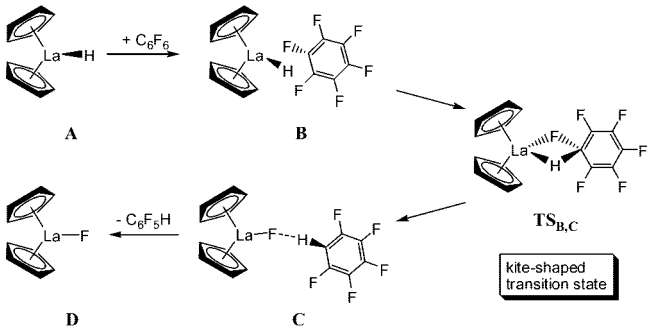

the orginal Cp_2LaH/C_6F_6 system and the recent Cp*(^{t}Bu$_3$P═N)TiH system (Scheme 1).

We will begin with the results for the kite-shaped transition state in the direct H/F exchange between Cp_2La and C_6F_6 by using different density functionals and basis sets. Then, the detailed mechanisms for the reactions of the cationic Ti system are described at the theoretical level of nonempirical meta-GGA Tao−Perdew−Staroverov−Scuseria[5] (TPSS) functional and all-electron correlation-consistent polarized valence double-ζ[6] (cc-pVDZ) basis set.

2. Computational Details

All calculations were performed using the Gaussian 03 suite of ab initio programs.[7] For the La system, TPSS, B3LYP,[8,9] and B3PW91[8,10] functionals with two rather large basis set settings: BS1 (6-311++G** basis sets for the H, C, and F atoms,[11] Stuttgart relativistic small core segmented ECP basis set for La,[12] and 675 basis functions and 1174 primitive Gaussians for $Cp_2La + C_6F_6$) and BS2 (cc-pVDZ basis sets for the H, C, and F atoms, Stuttgart relativistic small core segmented ECP basis set for La,[12] and 477 basis functions and 1086 primitive Gaussians for $Cp_2La + C_6F_6$). For the calculations on the cationic Ti system, the TPSS functional with cc-pVDZ basis set for H, C, N, P, and Cl atoms and cc-pVTZ basis set for Ti[13] was used (750 basis functions and 1988 primitive Gaussians for $\mathbf{1} + C_6H_5Cl$). Since the calculated energy barriers are very close to the experimental results, we believe the TPSS functional with current all-electron basis sets is a good choice for this molecular system.

Calculating the harmonic vibrational frequencies and noting the number of imaginary frequencies confirmed the nature of all intermediates (no imaginary frequency) and transition state structures (only one imaginary frequency). The latter were also confirmed to connect reactants and products by intrinsic reaction coordinate calculations. The zero-point energy and entropic contribution have been estimated within the harmonic potential approximation. The enthalpy, H, was calculated for $T = 298.15$ K. All relative enthalpies are reported in kcal/mol, based on separated reagents, which are set equal to 0.0 kcal/mol. The counterpoise method[14] was use to correct for the basis set superposition error (BSSE). The effect of solvent is taken into account by performing reaction field calculations using integral equation formalism polarizable continuum models (IEF-PCM) for the tetrahydrofuran (THF) solvent. The molecular structure figures displayed below are drawn by using the JIMP2 molecular visualization and manipulation program.[15]

3. Results and Discussion

3.1. H/F Exchange between Cp_2LaH and C_6F_6. The reaction pathway of direct H/F exchange between Cp_2LaH and C_6F_6 is displayed in Scheme 2. Cp_2LaH and C_6F_6 can attract each other to form a weak complex, intermediate **B** (Figure 1), then through a kite-shaped transition state $\mathbf{TS_{B,C}}$ (Figure 2), H and F can be exchanged directly to form another intermediate **C** with much lower energy. Then, from **C**, Cp_2LaF and C_6F_5H separate easily. In $\mathbf{TS_{B,C}}$, the phenyl ring is nearby coplanar with the line connecting the two centers of the Cp rings. The La, H, C, and F atoms form a nearby rhombic plane with a dihedral angel of 0.08° and almost perpendicular to the phenyl ring. Calculations with different density functionals and basis sets indicate that $Cp_2LaF + C_6F_5H$ is ~90 kcal/mol more stable than $Cp_2LaH + C_6F_6$, which is close to the 90.2 kcal/mol free energy difference obtained theoretically by Maron et al.[4] We were able to locate the kite-shaped transition state with all of the functionals and basis sets. Surprisingly, the energy barriers of this kite-shaped transition state are less than 10 kcal/mol higher than **B** (Table 1) in free energy, much lower than the 38.0 kcal/mol free energy barrier of the H/F exchange via HF formation proposed previously by Maron et al.[4] This low-energy barrier confirms the existence of a kite-shaped transition state in the reaction pathway of the H/F exchange between Cp_2LaH and C_6F_6. Therefore, the reaction mechanism proposed by Ma et al.[3] for the H/X exchange between cationic titanium hydride and halobenzene needs to be reevaluated.

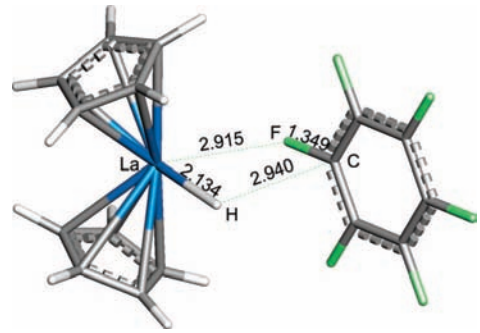

Figure 1. Optimized structure of intermediate **B** for the direct H/F exchange between Cp_2LaH and C_6F_6 by using the B3PW91 functional with BS1. Bond lengths are in angstroms.

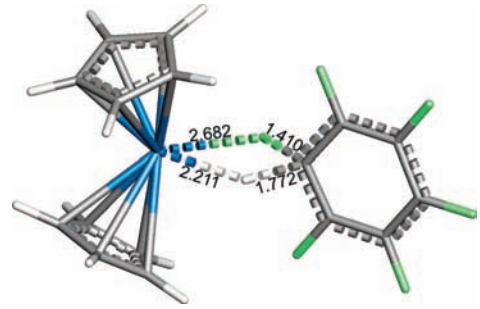

Figure 2. Optimized structure of the kite-shaped transition state $\mathbf{TS_{B,C}}$ (606.0i cm^{-1}) for the direct H/F exchange between Cp_2LaH and C_6F_6 by using the B3PW91 functional with BS1. Bond lengths are in angstroms. The La−H−C−F dihedral angle is only 0.08°.

3.2. H/Cl Exchange between 1 and C_6H_5Cl. The structures and calculated relative enthalpies of all complexes in the reactions between chlorobenzene and the cationic titanium hydride complex, including the direct H/Cl exchange by kite-shaped transition state (**2a** → **2Cl**), H_2 formation via *ortho*-C−H activation (**2a** → **2b**), H_2 release (**2b** → **2Cl**), and indirect C−Cl activation via β-halogen elimination (**3Cl** → **4Cl**), are displayed in Scheme 3. Figure 3 displays the kite-shaped transition state $\mathbf{TS_{2a,2c}}$ for the direct exchange of H and Cl between **1** and C_6H_5Cl. In this transition state, the Ti, H, C2,

TABLE 1: Calculated Gas-Phase Relative Energies of the Direct H/F Exchange between Cp_2LaH and C_6F_6 with a Kite-Shaped Transition State

	B3LYP/BS1			B3PW91/BS1			TPSS/BS1			B3PW91/BS2		
	ΔE	ΔH	ΔG	ΔE	ΔH	ΔG	ΔE	ΔH	ΔG	ΔE	ΔH	ΔG
A	0.00	0.00	0.00	0.00	0.00	0.00	0.00	0.00	0.00	0.00	0.00	0.00
B	−5.88	−4.58	4.75	−4.46	−3.15	5.89	−5.49	−4.13	5.34	−7.71	−6.54	2.42
$TS_{B,C}$	1.83	2.18	13.84	2.15	2.55	12.76	−1.12	−0.71	11.94	−0.70	−0.41	11.43
C	−93.80	−89.34	−81.77	−91.62	−89.04	−75.74	−91.38	−87.05	−78.95	−97.05	−92.96	−84.33
D	−89.24	−87.31	−84.16	−87.71	−85.86	−83.64	−86.52	−84.61	−81.56	−87.86	−85.49	−85.88

SCHEME 3: Predicted Mechanism and Relative Enthalpies (kcal/mol) in the Gas-Phase Reactions of Chlorbenzene at the Cationic Titanium Center, Including the Direct H/Cl Exchange by Kite-Shaped Transition State (2a → 2Cl), H_2 Formation by *ortho*-C−H Activation (2a → 2b), H_2 Release (2b → 2Cl), and the *β*-Halogen Elimination Reactions (3Cl → 4Cl)

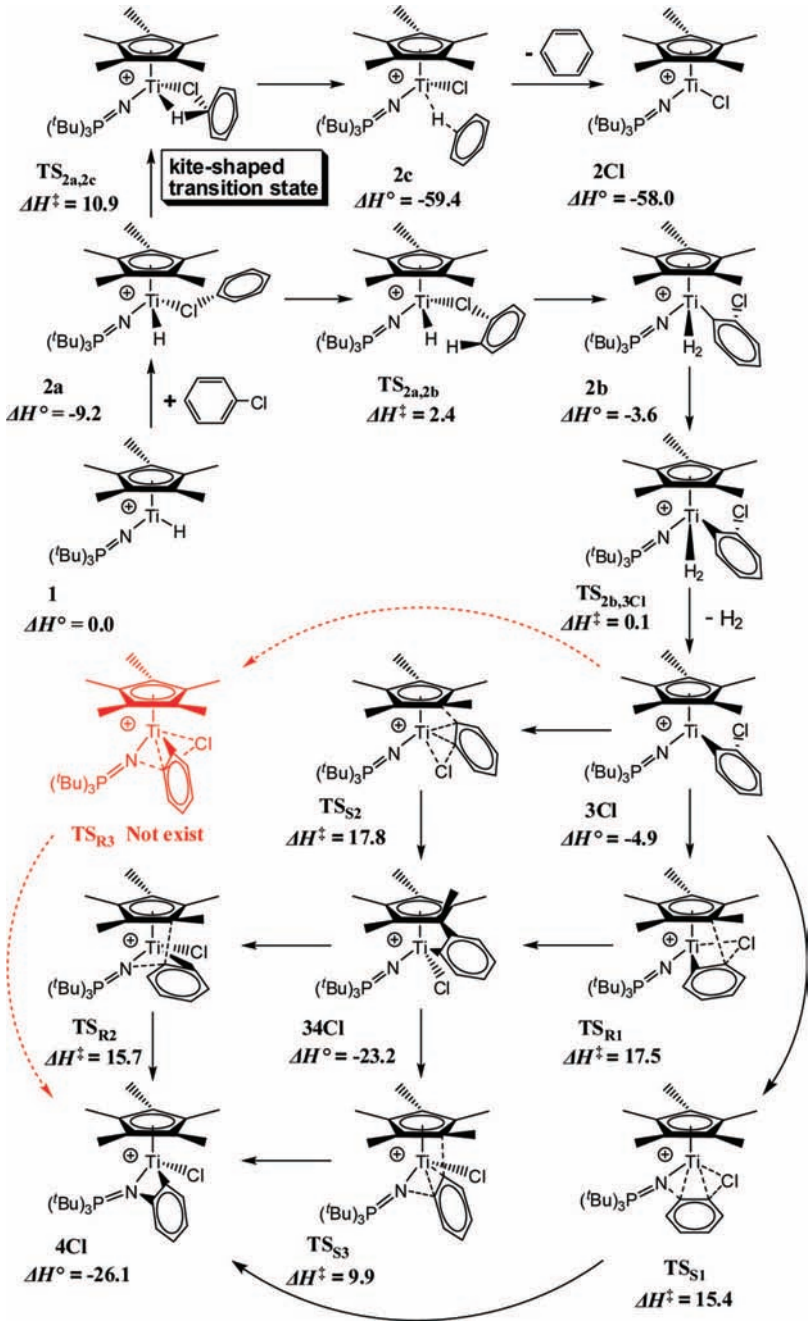

and Cl atoms form an approximate rhombic plane with only a 2.2° dihedral angle, the difference between the Ti−H and C−H bond lengths in this plane is only 0.01 Å, and this plane is almost perpendicular to both the Ti−N bond and the phenyl plane. The relative enthalpy of $TS_{2a,2c}$ is only 20.1 kcal/mol higher than that of **2a**; thus, this H/Cl exchange can occur under relatively mild conditions. Attempts to find a different transition state similar to that reported by Maron et al. for Cp_2LaH and C_6F_6,

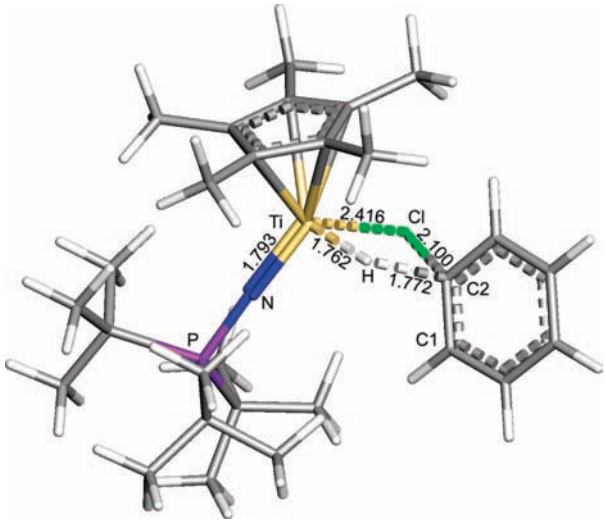

Figure 3. Optimized structure of the kite-shaped transition state $\mathbf{TS_{2a,2c}}$ (1193.1*i* cm^{-1}) for the direct H/Cl exchange. Bond lengths are in angstroms. The Ti−H−C2−Cl dihedral angle is only 2.2°.

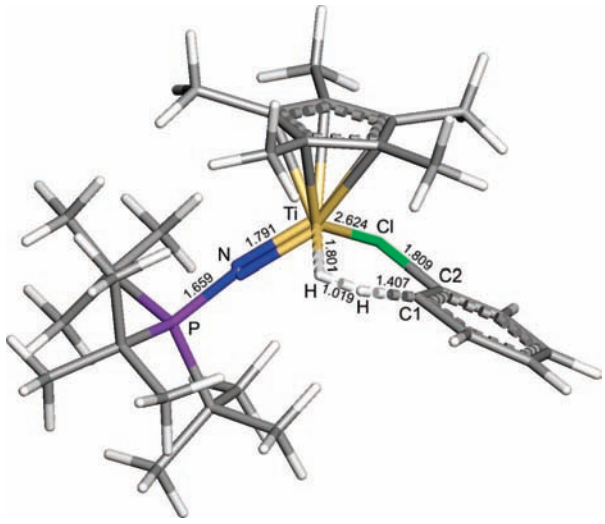

Figure 4. Optimized structure of transition state $\mathbf{TS_{2a,2b}}$ (965.4*i* cm^{-1}) for the formation of H_2 via the *ortho*-C−H activation. Bond lengths are in angstroms.

which in this case would produce a HCl intermediate, failed. To avoid postulating the kite-shaped transition state, Ma et al.[3] suggested a radical chain reaction pathway that invokes nucleophilic attack on the aryl halide followed by β-halo transfer to the metal. Although some H/Cl exchange could proceed by this route, the alternative kite-shaped transition state should provide a more competitive route.

3.3. Formation of 3Cl through the *ortho*-C−H Activation. Although the kite-shaped transition state is achievable under mild condition, there is another reaction pathway starting from **2a** through an *ortho*-C−H activation transition state $\mathbf{TS_{2a,2b}}$ to form an unstable intermediate **2b** with a dihydrogen bonding to Ti (Figure 4). Since the bond between Ti and H_2 in complex **2b** is very weak (3.7 kcal/mol), at lower H_2 pressure (>1 atm), **2b** will release H_2 rapidly and generate the observed intermediate **3Cl**. For these two transition states, the relative enthalpy of $\mathbf{TS_{2a,2b}}$ is 8.5 kcal/mol lower than that of $\mathbf{TS_{2a,2c}}$. This difference in enthalpic barriers explains why the direct H/Cl exchange reaction occurs only under high concentrations of H_2, which drives the kinetically favored complex **3Cl** back toward **1**.

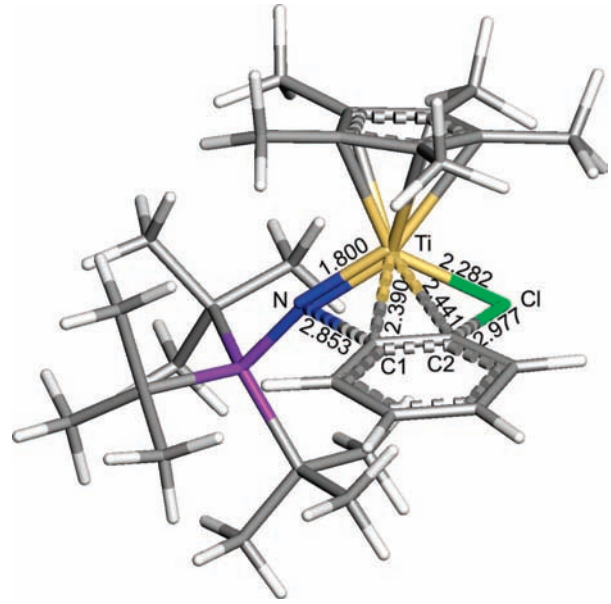

Figure 5. Optimized structure of the transition state $\mathbf{TS_{S1}}$ (126.2*i* cm^{-1}) for the formation of **4Cl** from **3Cl** in the β-halogen elimination process. Bond lengths are in angstroms.

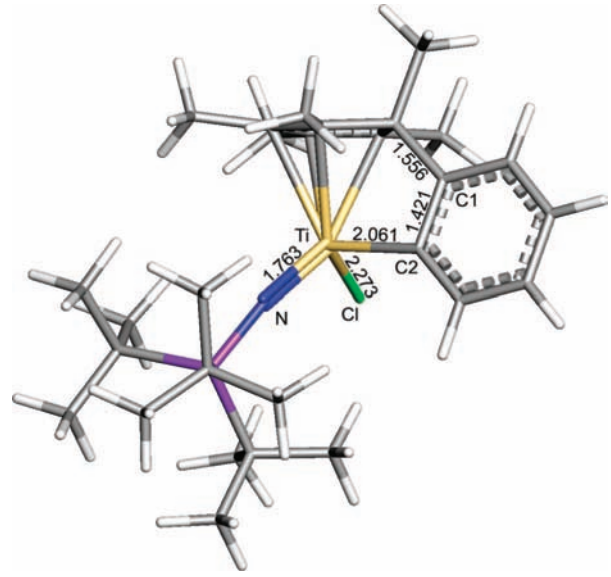

Figure 6. Optimized structure of stable complex **34Cl** from $\mathbf{TS_{S2}}$ in the β-halogen elimination process. Bond lengths are in angstroms.

3.4. Formation of 4Cl through the β-Halogen Elimination from 3Cl. 3Cl is still not very stable and will convert to the final product **4Cl** through indirect C−Cl activation under moderate heating. This conversion involves a complicated series of steps. The phenyl ring has three ways to move toward more stable structures: (1) it can slide toward the N atom creating transition state $\mathbf{TS_{S1}}$ (Figure 5) and forming **4Cl** in one step; (2) it can slide toward the Cp* and form the stable structure **34Cl** (Figure 6) through transition state $\mathbf{TS_{S2}}$ (Figure 7, C1 moves up and bonds with a C atom of Cp* while C2 leaves Cl and bonds with Ti); and (3) C1 (the carbon atom bound to Ti in **3Cl**) remains bound to Ti and C2 (the carbon atom bonded to Cl in **3Cl**) moves up (the phenyl plane rotates along the C1−Ti bond) and bonds with a carbon atom of Cp* through transition state $\mathbf{TS_{R1}}$ (Figure 8). This movement also forms the stable structure **34Cl**. **34Cl** is a structurally unusual isomer of the final product **4Cl** with a phenyl ring bridging the Cp* ring and metal center. Structures similar to that of **34Cl** have been

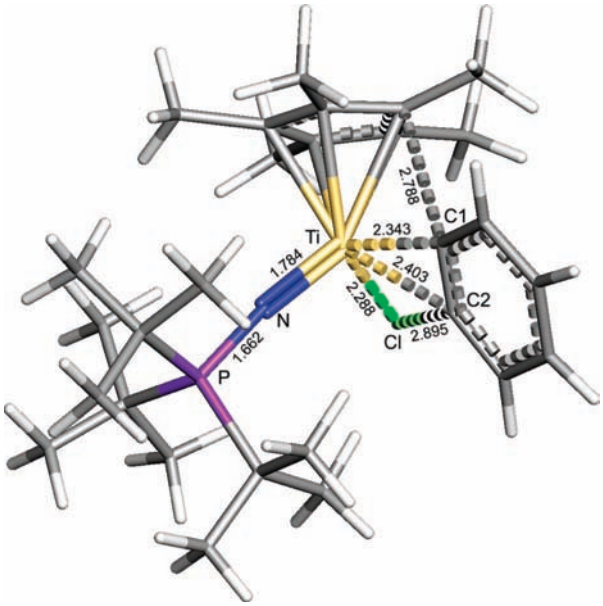

Figure 7. Optimized structure of the transition state $\mathbf{TS_{S2}}$ (128.1*i* cm^{-1}) for the formation of **34Cl** from **3Cl** in the β-halogen elimination process. Bond lengths are in angstroms.

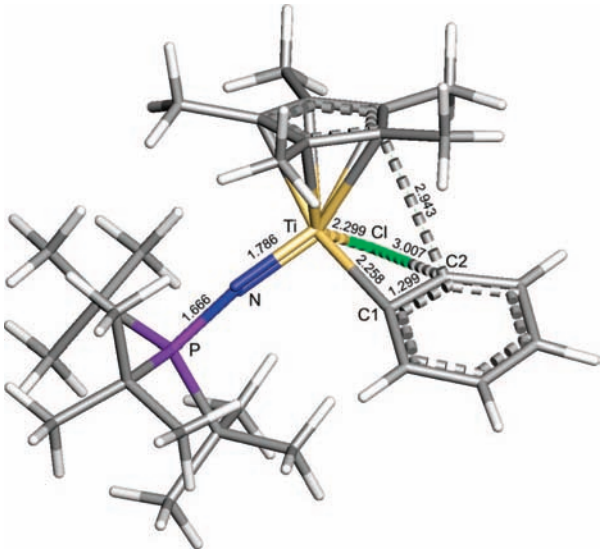

Figure 8. Optimized structure of the transition state $\mathbf{TS_{R1}}$ (91.1*i* cm^{-1}) for the formation of **34Cl** from **3Cl** in the β-halogen elimination process. Bond lengths are in angstroms.

obtained in $Cp^*_2ZrCl(C_6H_4)$ complexes by Wu et al.[16] However, this structure has yet to be observed in these Ti experiments. According to our calculations, the enthalpic barrier for **3Cl** → $\mathbf{TS_{S1}}$ is 20.3 kcal/mol, very close to the observed enthalpic barrier of 19.7 kcal/mol. The relative enthalpy of the transition state $\mathbf{TS_{S1}}$ is 2.1 and 2.4 kcal/mol lower than those of $\mathbf{TS_{S2}}$ and $\mathbf{TS_{R1}}$. Thus, the formation rate of **4Cl** is much faster than the formation rate of **34Cl**. Although the enthalpic barriers (33.1 and 38.9 kcal/mol for $\mathbf{TS_{S3}}$ (Figure 9) and $\mathbf{TS_{R2}}$ (Figure 10)) from **34Cl** to **4Cl** are rather high, **34Cl** is still 2.9 kcal/mol less stable than **4Cl** in enthalpy and will convert to **4Cl** at a certain rate.

3.5. Discussion on the Hypothesized Transition State $\mathbf{TS_{R3}}$. One might expect that phenyl rotation in the allowed directions would produce transition state $\mathbf{TS_{R3}}$, connecting **3Cl** and **4Cl** directly (C1 remains bound to Ti and C2 moves down toward the N atom). This type of transition state was hypothesized for

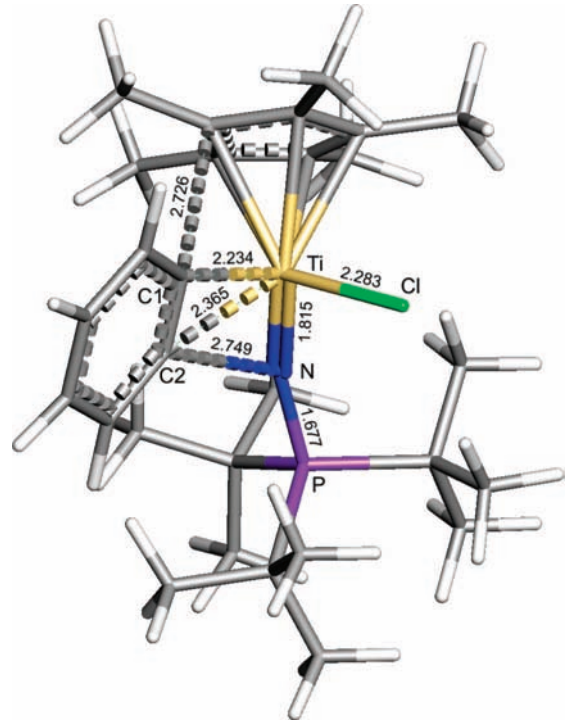

Figure 9. Optimized structure of the transition state $\mathbf{TS_{S3}}$ (79.8*i* cm^{-1}). Bond lengths are in angstroms.

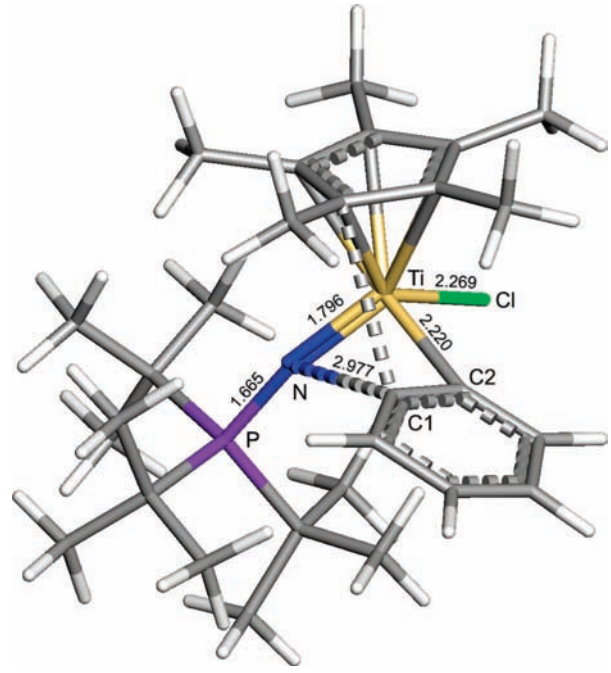

Figure 10. Optimized structure of the transition state $\mathbf{TS_{R2}}$ (64.5*i* cm^{-1}). Bond lengths are in angstroms.

the β-halogen elimination process by Ma et al.[3] However, all attempts to find this transition state failed because of the steric bulk of $^tBu_3P$ and Cp*; i.e., there is not enough space to allow the phenyl ring to make such a rotation. To verify this conjecture, we performed similar calculations on a simplified model $[Cp(Me_3P{=}N)Ti(2\text{-}Cl{-}C_6H_4)]^+$ (**3Cl′**), in which hydrogens replaced all methyl groups in **3Cl**. The rotary transition state$\mathbf{TS_{R3'}}$, which connects **3Cl′** and **4Cl′** directly, was now found (Figure 11). Thus, the selection of a suitable molecular model for the calculation of a complicated system is important to the details of the reaction mechanism. Generally, oversimpli-

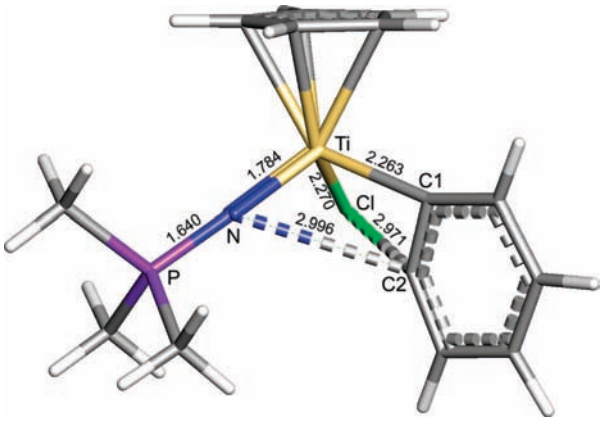

Figure 11. Optimized structure of the transition state $\mathbf{TS_{R3'}}$ ($87.5i$ cm^{-1}) for the formation of **4Cl′** from **3Cl′** in the β-halogen elimination process. Bond lengths are in angstroms. This type of transition state is obtained only for the simplified molecular model where all methyl groups were replaced by hydrogen atoms.

fied molecular structures can lead to unrealistic reaction pathways in some situation.

4. Conclusions

In conclusion, our calculations using different density functionals and basis sets demonstrate that the hydrogen on the metal center and halogen in halobenzene may exchange directly through the kite-shaped transition states, which previously were thought to have high energy barriers,[4] a prediction which misled others in proposing a mechanism for their recent experimental study.[3] Here, other halo−carbon activation pathways were found in the detailed mechanisms for the competitive reaction between a cationic titanium hydride complex and chlorobenzene under different H_2 pressures. The mechanism for the formation and release of H_2 has potential to be applied to other studies of hydrogen and C−H bond processes. A new stable structure, **34Cl**, which is an isomer of the final product **4Cl** with similar energy, contains a interesting bridging phenyl ring between the Cp* ring and metal center and was found in the indirect C−Cl activation via β-halogen elimination process. **34Cl** was not observed in experiments because the energy barrier of **3Cl** → **34Cl** is slightly higher than that of **3Cl** → **4Cl**. Finally, the effect of the oversimplification of the molecular model for complicated molecular systems in the theoretical study was discussed, and it was concluded that such simplifications can alter the energy barriers of key steps and lead to a different predicted mechanism.

Acknowledgment. This work was supported by grants from the NSF (CHE-0518074, CHE-0541587, and DMS-0216275) and the Welch Foundation (A0648).

Supporting Information Available: Atomic coordinates of optimized stationary points and transition states. This material is available free of charge via the Internet at http://pubs.acs.org.

References and Notes

(1) (a) Godula, K.; Sames, D. *Science* **2006**, *312*, 67. (b) Alberico, D.; Scott, M. E.; Lautens, M. *Chem. Rev.* **2007**, *107*, 174. (c) Bergman, R. G. *Nature* **2007**, *446*, 391.

(2) (a) Harrod, J. F. *Coord. Chem. Rev.* **2000**, *206−207*, 493. (b) Hoskin, A. J.; Stephan, D. W. *Coord. Chem. Rev.* **2002**, *233−234*, 107.

(3) Ma, K.; Piers, W. E.; Parvez, M. *J. Am. Chem. Soc.* **2006**, *128*, 3303.

(4) Maron, L.; Werkema, E. L.; Perrin, L.; Eisenstein, O.; Andersen, R. A. *J. Am. Chem. Soc.* **2005**, *127*, 279.

(5) Tao, J. M.; Perdew, J. P.; Staroverov, V. N.; Scuseria, G. E. *Phys. Rev. Lett.* **2003**, *91*, 146401.

(6) (a) Dunning, T. H., Jr *J. Chem. Phys.* **1989**, *90*, 1007. (b) Woon, D. E.; Dunning, T. H., Jr *J. Chem. Phys.* **1993**, *98*, 1358.

(7) Frisch, M. J.; Trucks, G. W.; Schlegel, H. B.; Scuseria, G. E.; Robb, M. A.; Cheeseman, J. R.; Montgomery, J. A., Jr.; Vreven, T.; Kudin, K. N.; Burant, J. C.; Millam, J. M.; Iyengar, S. S.; Tomasi, J.; Barone, V.; Mennucci, B.; Cossi, M.; Scalmani, G.; Rega, N.; Petersson, G. A.; Nakatsuji, H.; Hada, M.; Ehara, M.; Toyota, K.; Fukuda, R.; Hasegawa, J.; Ishida, M.; Nakajima, T.; Honda, Y.; Kitao, O.; Nakai, H.; Klene, M.; Li, X.; Knox, J. E.; Hratchian, H. P.; Cross, J. B.; Adamo, C.; Jaramillo, J.; Gomperts, R.; Stratmann, R. E.; Yazyev, O.; Austin, A. J.; Cammi, R.; Pomelli, C.; Ochterski, J. W.; Ayala, P. Y.; Morokuma, K.; Voth, G. A.; Salvador, P.; Dannenberg, J. J.; Zakrzewski, V. G.; Dapprich, S.; Daniels, A. D.; Strain, M. C.; Farkas, O.; Malick, D. K.; Rabuck, A. D.; Raghavachari, K.; Foresman, J. B.; Ortiz, J. V.; Cui, Q.; Baboul, A. G.; Clifford, S.; Cioslowski, J.; Stefanov, B. B.; Liu, G.; Liashenko, A.; Piskorz, P.; Komaromi, I.; Martin, R. L.; Fox, D. J.; Keith, T.; Al-Laham, M. A.; Peng, C. Y.; Nanayakkara, A.; Challacombe, M.; Gill, P. M. W.; Johnson, B.; Chen, W.; Wong, M. W.; Gonzalez, C.; Pople, J. A. *Gaussian 03, suite of programs for ab initio calculation*, revision C.02; Gaussian, Inc.: Wallingford, CT, 2004.

(8) Becke, A. D. *J. Chem. Phys.* **1993**, *98*, 5648.

(9) Lee, C.; Yang, W.; Parr, R. G. *Phys. Rev. B* **1988**, *37*, 785.

(10) (a) Burke, K.; Perdew, J. P.; Wang, Y. In *Electronic Density Functional Theory: Recent Progress and New Directions*; Dobson, J. F., Vignale, G., Das, M. P., Eds.; Plenum: New York, 1998; pp 81−111. (b) Perdew, J. P. In *Electronic Structure of Solids ′91*; Ziesche, P., Eschrig, H., Eds.; Akademie Verlag: Berlin, 1991; p 11. (c) Perdew, J. P.; Chevary, J. A.; Vosko, S. H.; Jackson, K. A.; Pederson, M. R.; Singh, D. J.; Fiolhais, C. *Phys. Rev. B* **1992**, *46*, 6671. (d) Perdew, J. P.; Chevary, J. A.; Vosko, S. H.; Jackson, K. A.; Pederson, M. R.; Singh, D. J.; Fiolhais, C. *Phys. Rev. B* **1993**, *48*, 4978. (e) Perdew, J. P.; Burke, K.; Wang, Y. *Phys. Rev. B* **1996**, *54*, 16533.

(11) (a) McLean, A. D.; Chandler, G. S. *J. Chem. Phys.* **1980**, *72*, 5639. (b) Krishnan, R.; Binkley, J. S.; Seeger, R.; Pople, J. A. *J. Chem. Phys.* **1980**, *72*, 650.

(12) (a) Balabanov, N. B.; Peterson, K. A. *J. Chem. Phys.* **2005**, *123*, 064107. (b) Balabanov, N. B.; Peterson, K. A. *J. Chem. Phys.* **2006**, *125*, 074110.

(13) Balabanov, N. B.; Peterson, K. A. *J. Chem. Phys.* **2005**, *123*, 064107.

(14) (a) Boys, S. F.; Bernardi, F. *Mol. Phys.* **1970**, *19*, 553. (b) Simon, S.; Duran, M.; Dannenberg, J. J. *J. Chem. Phys.* **1996**, *105*, 11024.

(15) (a) JIMP2, version 0.091, a free program for visualizing and manipulating molecules. Hall, M. B.; Fenske, R. F. *Inorg. Chem.* **1972**, *11*, 768. (b) Manson, J.; Webster, C. E.; Hall, M. B. Texas A&M University, College Station, TX, 2006.

(16) Wu, F.; Dash, A. K.; Jordan, R. F. *J. Am. Chem. Soc.* **2004**, *126*, 15360.

JP809272Y